Congrès Français de Mécanique - 2019

DYNAMIC RESPONSE OF POROUS DUCTILE MATERIALS CONTAINING CYLINDRICAL VOIDS

Manoj Subramani, Christophe Czarnota , Sébastien Mercier and Alain Molinari

[1]*Université de Lorraine, CNRS, Arts et Métiers ParisTech, LEM3, 7 rue Felix savart, 57073 Metz Cedex 03, France.*

manoj.subramani@univ-lorraine.fr christophe.czarnota@univ-lorraine.fr sebastien.mercier@univ-lorraine.fr alain.molinari@univ-lorraine.fr

Keywords: Dynamic homogenization, micro-inertia, length-scale effect, damage, porous material

1 Introduction

The fracture of ductile materials is often the result of the nucleation, growth and coalescence of microscopic voids. In this work, we focus on the growth process of voids when the material is subjected to high strain rate loading. Under such loading conditions, micro-voids sustain an extremely rapid expansion which generates strong acceleration of particles in the vicinity of cavities. These micro-inertia effects are thought to play an important role in the development of dynamic damage. To account for these large accelerations in the constitutive behavior, a multi-scale approach has been proposed in [1]. Up to now, micro inertia effects were mainly evaluated for porous materials containing spherical or spheroidal voids. In the present talk, we are focusing on the description of the behavior of a porous material with cylindrical voids under dynamic conditions. Note that such a configuration was already considered in [2], but the contribution of the acceleration in the direction aligned with the axis of the cylinder was disregarded. This formalism leads to neglect the influence of the length of the cylinder on the dynamic response, which may be too restrictive in some situations. Here, we propose to investigate the dynamic expansion of cylindrical voids under axi-symmetric loading conditions. The present modeling includes two length scale effects: the one related to the initial void radius, and the one brought by the initial length of the voids. The results obtained from the modeling are validated through comparison with finite element calculations conducted on a unit cell (Abaqus/Explicit). Within the present approach, the effects of the initial length of the voids on the macroscopic response are clearly highlighted.

2 Modeling

To derive the constitutive model for a porous material with cylindrical voids, a multiscale approach founded on the work of Molinari and Mercier [1] is adopted here. Under dynamic loading, when micro-inertia effects need to be accounted for, the macroscopic stress can no longer be defined as the volume average of the local stress (static definition). In fact, due to large acceleration developed at the local scale, the macroscopic stress stress tensor Σ appears as the sum of two contributions: micro-inertia independent term Σ^{stat} and a dynamic term (micro-inertia dependent term) Σ^{dyn} :

$$\Sigma = \Sigma^{stat} + \Sigma^{dyn} \tag{1}$$

In our approach Σ^{stat} will be derived from the Gurson model [3]. The Σ^{dyn} tensor will be evaluated based an admissible trial velocity fields proposed by Gurson [3].

2.1 Representative Volume Element (RVE)

In this work, the focus is on the dynamic response of porous medium with cylindrical voids. The RVE, similar to the one proposed by Gurson [3], respectively consists of a hollow cylinder of current inner radius a, outer radius b, length L, see Fig. 1. The corresponding initial geometrical features are a_0, b_0 and L_0. The current and initial porosity are given by $f = \left(\frac{a}{b}\right)^2$ and $f_0 = \left(\frac{a_0}{b_0}\right)^2$.

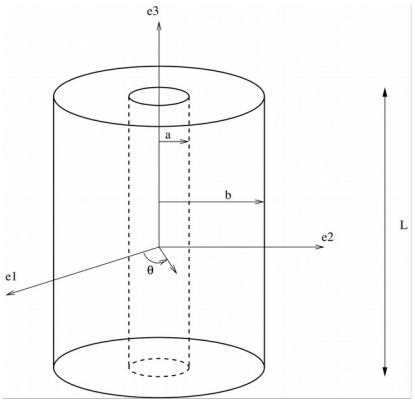

Fig 1: RVE (Representative Volume Element) for a porous material containing cylindrical void.

The matrix surrounding the cylindrical cavity is assumed incompressible and elasticity is neglected. So the time evolution of the porosity is thus:

$$\dot{f} = 3(1-f)D_m \tag{2}$$

where $D_m=(trD)/3$, where tr (.) is the trace of second order tensor (.).

In the present talk, the material is assumed perfectly plastic with σ_0 standing for the matrix yield stress. The RVE is subjected to transversely isotropic loading conditions. In that case, the macroscopic stress and strain rate tensors are written in the orthonormal frame basis ($\mathbf{e_1}$, $\mathbf{e_2}$, $\mathbf{e_3}$) as, see Fig.1:

$$\Sigma = \begin{bmatrix} \Sigma_{11} & 0 & 0 \\ 0 & \Sigma_{11} & 0 \\ 0 & 0 & \Sigma_{33} \end{bmatrix} \quad \text{and} \quad D = \begin{bmatrix} D_{11} & 0 & 0 \\ 0 & D_{11} & 0 \\ 0 & 0 & D_{33} \end{bmatrix} \tag{3}$$

2.2 Micro-inertia independent stress, Σ^{stat} and Micro- inertia dependent stress, Σ^{dyn}

The static stress tensor Σ^{stat} of Eq. (1) is derived from the yield function proposed by Gurson [3] for cylindrical voids. Under axi-symmetric loading, the yield function $\Phi\left(\Sigma^{stat},\sigma_0,f\right)$, is expressed as:

$$\Phi\left(\Sigma^{stat},\sigma_0,f\right) = \left(\frac{\Sigma_{eq}^{stat}}{\sigma_0}\right)^2 + 2f\cosh\left(\sqrt{3}\frac{\Sigma_{11}^{stat}}{\sigma_0}\right) - \left(1+f^2\right) = 0 \quad , \quad \Sigma_{eq}^{stat} = \sqrt{\frac{3}{2}\Sigma^{stat'}:\Sigma^{stat'}} \tag{4}$$

where (.)' denotes the deviatoric part of the second order tensor (.) and ':' stands for the double contracted product. For axi-symmetric loading, the stress and strain rate tensors are related by explicit expressions, [8]. In this case:

$$\Sigma_{11}^{stat} = \Sigma_{22}^{stat} = \sigma_0\beta_1 \quad , \quad \Sigma_{33}^{stat} = \sigma_0\left(\beta_1+\beta_2\right) \tag{5}$$

where, $\beta_1 = \frac{1}{\sqrt{3}}\ln\left(X+\sqrt{X^2-1}\right)sgn\left(D_m\right)$, $\beta_2 = \frac{D_{33}}{\sqrt{3}D_m}f\sinh\left(\sqrt{3}\beta_1\right)$

with $X = \dfrac{-1+\sqrt{1+3\left(\frac{D_{33}}{3D_m}\right)^2\left(1+f^2+3f^2\left(\frac{D_{33}}{3D_m}\right)^2\right)}}{3\left(\frac{D_{33}}{3D_m}\right)^2 f}$

The plane strain configuration where $D_{33}=0$ (i.e. the length of the cylinder remains constant $L=L_0$) is also treated in the paper. In that case, Eq. (5) reduce to

$$\Sigma_{11}^{stat} = \Sigma_{22}^{stat} = \Sigma_{33}^{stat} = \frac{1}{\sqrt{3}}\sigma_0\ln\left(\frac{1}{f}\right)sgn\left(D_{11}\right) \tag{6}$$

Note from Eqs (1, 6) that when micro-inertia is neglected and the plane strain case ($D_{33}=0$) is adopted, the stress tensor is hydrostatic given in Eq. 6. However, this is no more valid when micro-inertia is included.

For sake of brevity, the dynamic stress tensor Σ^{dyn} of Eq. (1) is put in a condensed form. In the case of axi-

symmetric loading, the components of Σ^{dyn} are written as:

$$\Sigma_{11}^{dyn}=\Sigma_{22}^{dyn}=\rho a^2 F\,,\Sigma_{33}^{dyn}=\rho a^2 G+\rho L^2\left(\frac{1-f}{3}\right)\left(\dot{D}_{33}+D_{33}^2\right) \tag{7}$$

where F and G are functions depending on the porosity f, quadratic terms involving D_{11} and D_{33}, and linear terms implying the time derivatives $\dot{D}_{11}$ and $\dot{D}_{33}$. This confirms the particular rate dependencies brought by the micro-inertia to the overall response, already noticed for spherical and spheroidal voids [1,4]. Eq. (7) also reveals that the dynamic stress is scaled by the matrix mass density and involves the square of the void radius and the void length. More specifically, an important outcome of the model is the differential lengthscale effect which exists between in plane and axial components of the macroscopic stress. Namely, it is observed that the in plane stress components $\Sigma_{11}^{dyn}=\Sigma_{22}^{dyn}$ are only related to the square of the void radius while Σ_{33}^{dyn} is linked to the square of the void radius a^2 and the square of the void length L^2. In the plane strain case, D_{33}=0, the following explicit relationships are obtained:

$$\begin{aligned}\Sigma_{11}^{dyn}=\Sigma_{22}^{dyn}&=\frac{\rho a^2}{2}\left(f^{-1}\ln\left(\frac{1}{f}\right)\dot{D}_{11}-f^{-1}\left(f^{-1}-2\ln\left(\frac{1}{f}\right)-1\right)D_{11}^2\right)\\ \Sigma_{33}^{dyn}&=\frac{\rho a^2}{2}\left(\left(f^{-1}\ln\left(\frac{1}{f}\right)-f^{-1}+1\right)\dot{D}_{11}-\left((1+f)f^{-2}-3f^{-1}\ln\left(\frac{1}{f}\right)-2\right)D_{11}^2\right)\end{aligned} \tag{8}$$

Interestingly, Eq. (8) show that micro-inertia effects are still present in Σ_{33}^{dyn}. This means that limiting the analysis to a 2D plane configuration, thus ignoring these effects, may leave aside substantial information on the role played by micro-inertia.

3. Results

We consider the dynamic response of a porous medium with cylindrical voids (initial void radius a_o=50μm, initial external radius b_0=1500μm, leading to $f_0\approx 1{,}1\,x10^{-3}$). Various values of the initial length of the cylinder are considered. The matrix parameters are $\sigma_0=100\,MPa$, $\rho=2700\,kg/m^3$. The porous material is subjected to dynamic loading leading to void expansion. The following distinct loading conditions are considered:

- spherical loading where the stress components are prescribed: $\Sigma_{11}=\Sigma_{22}=\Sigma_{33}=\dot{p}\,t$.
- axi-symmetric loading where D_{33}=0 is imposed and $\Sigma_{11}=\Sigma_{22}=\dot{p}\,t$ are prescribed.

In the following, a constant value of stress ramp is adopted: $\dot{p}=10\,MPa/ns$. In addition, once a critical porosity is reached (here taken as 0.3), the failure of the material is assumed to occur with no coalescence stage. This type of ultimate failure mechanism (direct impingement) will occur in ductile materials when submitted to planar impact experiments [6,7]. Note that results obtained from our analytical modeling have been accurately compared to unit cell calculations conducted using Abaqus/Explicit (not shown here). Moreover, for the cases treated in the paper, we have noticed a perfect match between the modeling and numerical simulations, thus validating the analytical approach.

Fig. 2 presents the time evolution of the porosity for the spherical loading condition, considering the static case (micro-inertia is disregarded) and the case where micro-inertia is included. In our work, the initial length of void L_0 is varied in the range [1; 20,000]μm. One first notes the strong influence of micro-inertia. Indeed, under static loading, the failure is occurring at a critical time $t_c=\sigma_0/\left(\sqrt{3}\,\dot{p}\right)\ln\left(1/f_0\right)=39.2\,ns$. This value is much lower than the critical time revealed when local dynamic effects are included. As an example, the complete failure occurs at 920ns when L_0=1000μm. This clearly illustrates the stabilizing effect of micro-inertia. Fig. 2 also reveals that the time to failure is increased as L_0 is increased. When L_0 becomes large, the response is tending to the case where D_{33}=0. An asymptotic response is also revealed when L_0 tends to zero.

Fig. 3 shows the time evolution of the macroscopic stress components $\Sigma_{11}=\Sigma_{22}$ (prescribed) and Σ_{33} calculated from the theory Eq. (8) where plane strain case is adopted. Remind that if micro-inertia is neglected, Σ_{33} coincide with $\Sigma_{11}=\Sigma_{22}$. From Fig. 3, it appears that the magnitude of the stress component Σ_{33} is increasing first, reaches a maximum and then decreases. Note that this Σ_{33} time evolution is confirmed by FE calculations. This finding, which could have been hardly anticipated without

the proposed analytical approach, clearly highlights the peculiar influence of the initial length and the role of micro-inertia in the dynamic response of porous materials containing cylindrical voids.

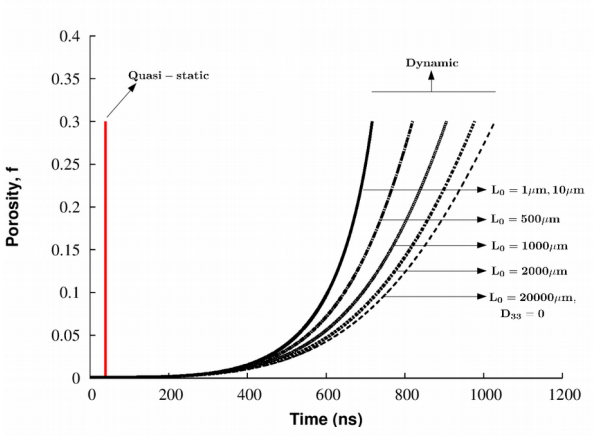

Fig 2: Porosity versus time for static (micro-inertia neglected) and dynamic approaches (including micro-inertia) for L_0=1 to 20,000µm. Spherical loading is considered.

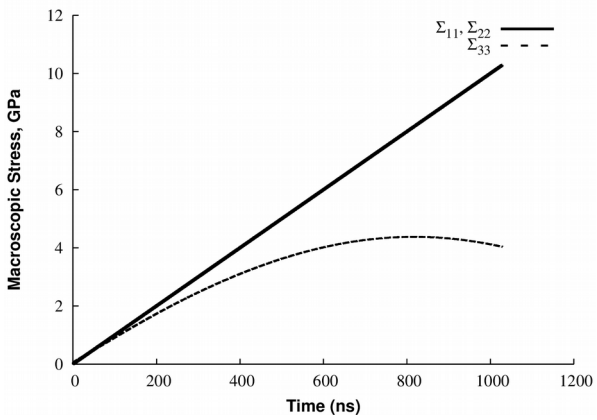

Fig 3: Macroscopic stress components $\Sigma_{11}=\Sigma_{22}$ (prescribed) and Σ_{33} (calculated) versus time when D_{33}=0. Micro-inertia is included.

Acknowledgements : The research conducted in this work has received funding from the European Union's Horizon 2020 Programme (Excellent Science, Marie-Sklodowska-Curie Actions) under REA grant agreement 675602 (OUTCOME Project).

References :

[1] A. Molinari, S. Mercier, (2001). Micro-mechanical modeling of porous materials under dynamic loading. J. Mech. Phys. Solids, 49, 1497-1516.

[2] Leblond, J.-B., & Roy, G. (2000). A model for dynamic ductile behavior applicable for arbitrary triaxialities. Comptes Rendus de l'Académie des Sciences- Series IIB – Mechanics, 328, 381 – 386A.

[3] L. Gurson, (1977). Continuum theory of ductile rupture by void nucleation and growth : Part I - yield criteria and flow rules for porous ductile media. J. Eng. Mater. Technol., 99, 2–15.

[4] C.Sartori, S.Mercier, N.Jacques, A. Molinari (2014). Constitutive behavior of porous ductile materials accounting for micro-inertia and void shape. Mechanics of Materials, 324-339.

[5] Leblond, J-B., Perrin, G., Suquet, P., 1994. Exact results and approximate models for porous visco-plastic solids, Int. J. Plast. 10, 213-235.

[6] Jacques, N., Czarnota, C., Mercier, S., & Molinari, A. (2010). A micromechanical constitutive model for dynamic damage and fracture of ductile materials. Int. J. Fract., 162, 159-175.

[7] Czarnota, C., Jacques, N., Mercier, S., & Molinari, A. (2008). Modelling of dynamic ductile fracture and application to the simulation of plate impact tests on tantalum. J. Mech. Phys. Solids, 56, 1624-1650.

[8] C.Sartori, S.Mercier, A. Molinari (2019). Analytical expression of mechanical fields for Gurson type porous models, International Journal of Solids and Structures, 163, 25-39.